The Abdus Salam
International Centre for Theoretical Physics

United Nations
Educational, Scientific and
Cultural Organization

IAEA
International Atomic Energy Agency

2332-2

School on Synchrotron and FEL Based Methods and their Multi-Disciplinary Applications

19 - 30 March 2012

Advances in energy dispersive X-ray absorption spectroscopy

S. Pascarelli
ESRF (France)

The Abdus Salam
International Centre for Theoretical Physics

United Nations
Educational, Scientific and
Cultural Organization

IAEA
International Atomic Energy Agency

School on Synchrotron and FEL Based Methods and their Multi-Disciplinary Applications

Trieste – Italy, 19-30 March 2012

Wednesday, 21 March 2012

14:00 – 15:30	**G. Aquilanti** / *Sincrotrone Trieste*
	XAS: principles
15:30 – 16:00	---BREAK---
16:00 – 18:30	**G. Aquilanti** / *Sincrotrone Trieste*
	XAS data analysis: (lecture with exercises)

Thursday, 22 March 2012

09:00 – 10:00	**S. Pascarelli** / *ESRF (France)*
	Advances in energy dispersive X-ray absorption spectroscopy
10:00 – 10:30	---BREAK---
10:30 – 11:30	**S. Pascarelli** / *ESRF (France)*
	Time resolved and high pressure science

Outline

XAS, XANES, EXAFS, and XMCD

- X-ray Absorption
- X-ray Absorption Fine Structure
- Simple Theoretical Description
- XANES
- Major historical EXAFS breakthroughs
- Applications of XAFS at ELETTRA
- EXAFS data analysis
- Introduction to XMCD

yesterday

Energy Dispersive XAS

- X-ray Absorption Spectrometers
- EDXAS
  - Basic principles, historical evolution
  - Examples of applications at ESRF
  - Future opportunities for studies of matter at extremes
- Probing laser induced extreme states of matter

today

Outline

XAS, XANES, EXAFS, and XMCD

- X-ray Absorption
- X-ray Absorption Fine Structure
- Simple Theoretical Description
- XANES
- Major historical EXAFS breakthroughs
- Examples of applications at ELETTRA
- EXAFS data analysis

- Introduction to XMCD

yesterday

today

Energy Dispersive XAS

- X-ray Absorption Spectrometers
- EDXAS
    - Basic principles, historical evolution
    - Examples of applications at ESRF
    - Future opportunities for studies of matter at extremes
- Probing laser induced extreme states of matter

Polarisation Dependent X-ray Spectroscopy: Dichroism

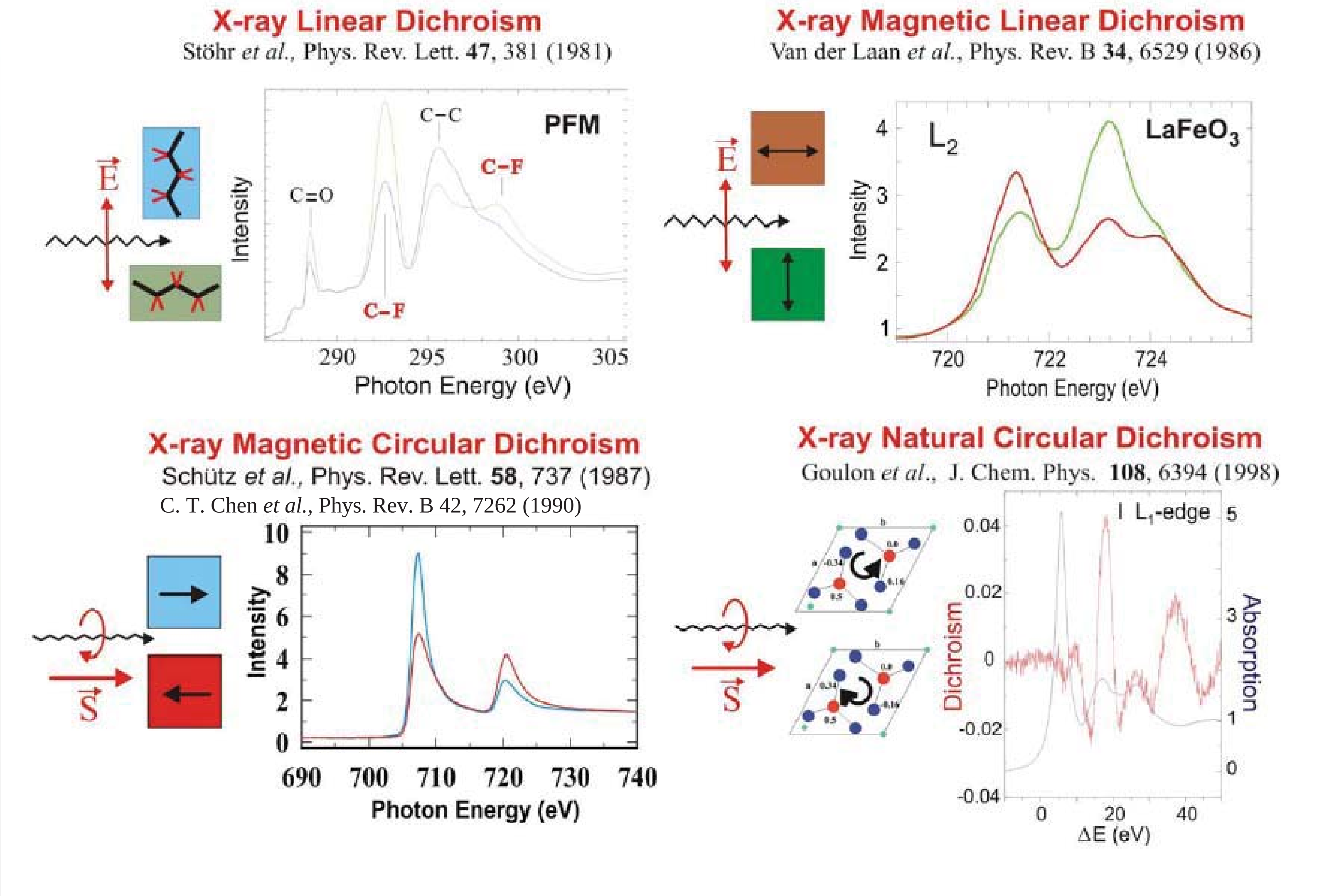

XLD: X-ray Linear Dichroism

dependence of absorption on the relative orientation between x-ray polarization and crystallographic axis

$$XLD = \frac{\mu^{//} - \mu^{\perp}}{\mu^{//} + \mu^{\perp}}$$

$\mu^{//} : \vec{E} \,//\, \vec{c}$

$\mu^{\perp} : \vec{E} \perp \vec{c}$

linearly polarized X-rays

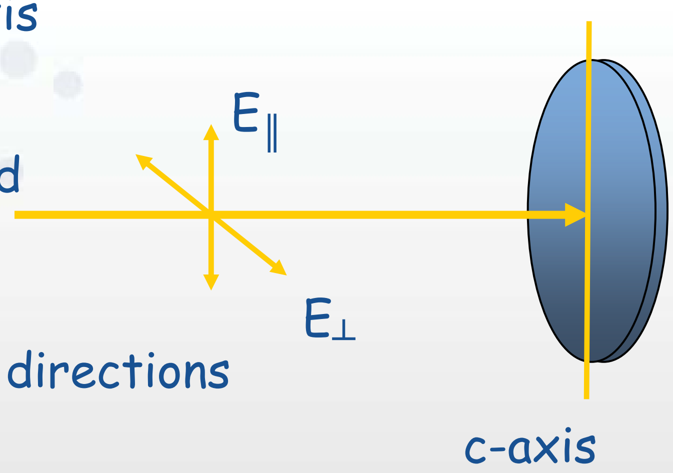

$\vec{E}$: search-light for no. of valence holes in different directions

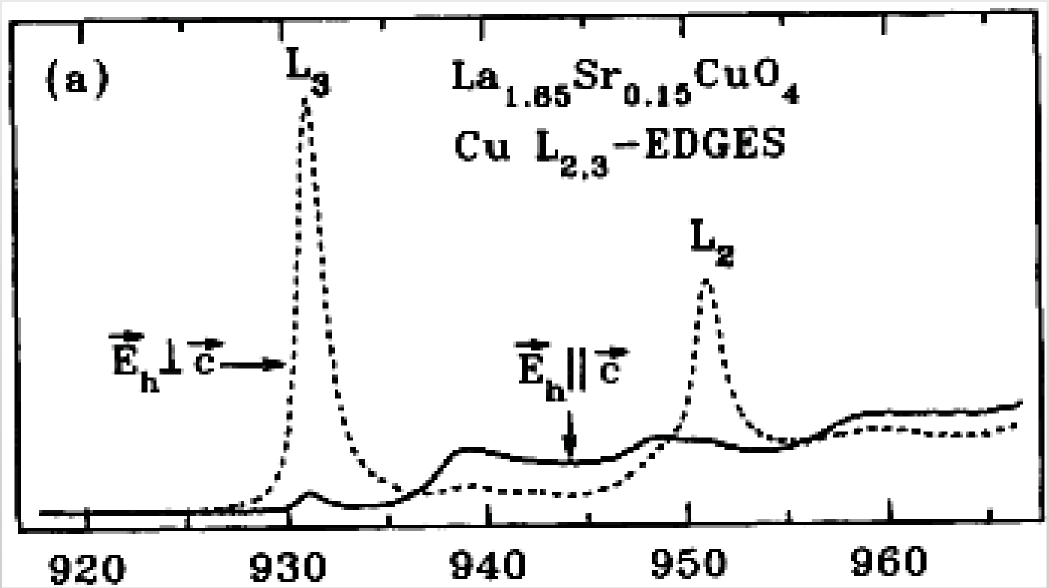

2p → 3d dipole allowed transition

The polarisation dependence gives the symmetry of the empty orbitals

C.T. Chen et al. PRL (1992)

XMLD: X-ray Magnetic Linear Dichroism

dependence of absorption on the relative orientation between
x-ray polarization and spin direction

$$XMLD = \frac{\mu^{//} - \mu^{\perp}}{\mu^{//} + \mu^{\perp}}$$

$\mu^{//}$: $\vec{E} \,//\, \vec{M}$

$\mu^{\perp}$: $\vec{E} \perp \vec{M}$

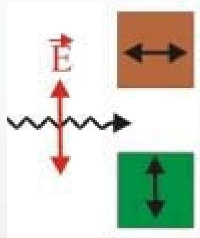

$\vec{E}$: search-light for no. of valence holes in different directions

❑ Absence of spin order: charge order in systems where the absorbing atom has lower than cubic symmetry (XLD)

❑ Presence of spin order: spin-orbit coupling leads to preferential charge order relative to the spin direction even in cubic systems

XMLD at absorption edge

spin axis direction in
(anti)ferromagnetic systems

XMLD in EXAFS region

local atomic displacements
around absorber atom

XMCD: X-Ray Magnetic Circular Dichroism

difference in absorption of left and right circularly polarized x-rays by a magnetic material

$$\text{XMCD} = \frac{\mu^L - \mu^R}{\mu^L + \mu^R}$$

μ^L : absorption coefficient using CPL

μ^R : absorption coefficient using CPR

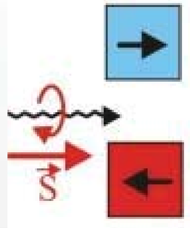

- ❑ Information on spin and orbital moment in magnetic materials
- ❑ To make the absorption process spin dependent:
  - ➢ circularly polarized photons
  - ➢ transfer their angular momentum to photoelectron

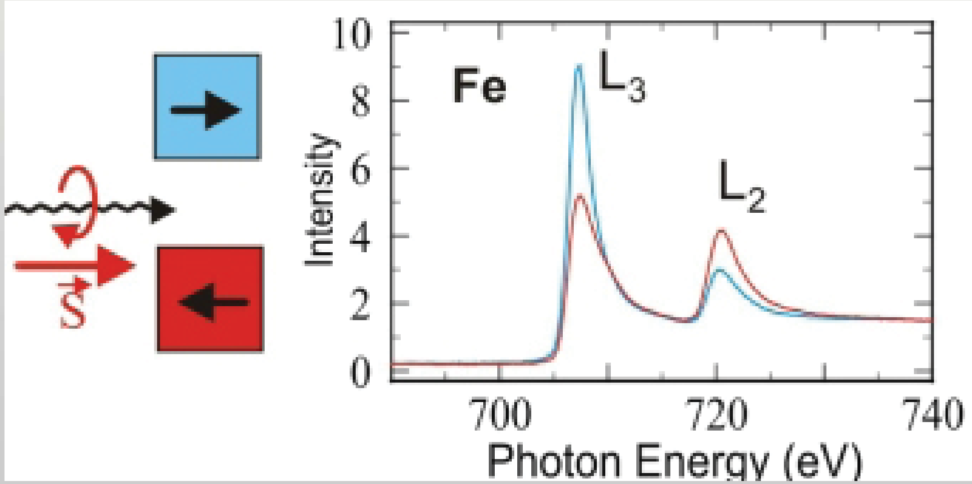

Fe $L_{2,3}$-edge XMCD

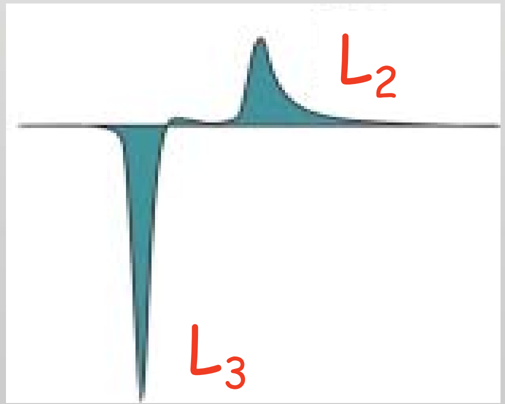

Main properties of XMCD

- Element selectivity
  i.e. iron, copper, platinum (induced magnetism)

- Orbital selectivity
  different edges of a same element → different valence electrons
  Fe: $L_{2,3}$ edges (2p → 3d) K edge (1s → 4p)

- Sum rules
  allow to obtain separately orbital and spin contributions to the magnetic moments from the integrated XMCD signal

- Sensitivity << 1ML
  impurities, very thin layers, adatoms on surfaces…

- High penetration depth for hard XMCD → allows to probe magnetism at extreme pressure

- XMCD relies on the presence of a net <M> along k
  Ferromagnetic, ferrimagnetic and paramagnetic systems can be probed

- XMCD can be used for element specific magnetic imaging

- Angular dependence → orbital moment anisotropy – magnetic anisotropy

The polarization dependent dipole operator

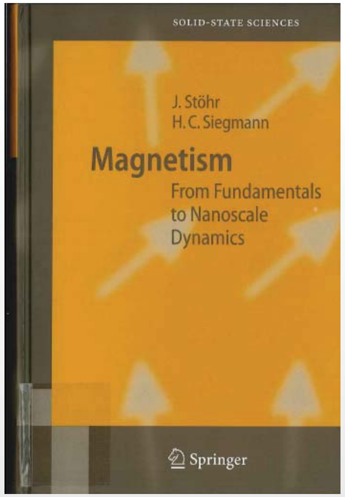

$$I_{\mathrm{res}} = \mathcal{A}\,|\langle b|\,\boldsymbol{\epsilon}\cdot \boldsymbol{r}|a\rangle|^2$$

dipole operator

$$P^q_\alpha = \boldsymbol{\epsilon}\cdot\mathbf{r} = \boldsymbol{\epsilon}^q_\alpha\cdot\mathbf{r}$$

α = x, y , z — X-ray prop direction

q = +1, 0, -1 — polarization states

($q\hbar$ photon angular momentum)

electron position vector $\mathbf{r} = x\mathbf{e}_x + y\mathbf{e}_y + z\mathbf{e}_z$

photon polarization vectors

$$\boldsymbol{\epsilon}^0_x = \boldsymbol{\epsilon}_x = \boldsymbol{e}_x \qquad \boldsymbol{\epsilon}^0_y = \boldsymbol{\epsilon}_y = \boldsymbol{e}_y \qquad \boldsymbol{\epsilon}^0_z = \boldsymbol{\epsilon}_z = \boldsymbol{e}_z$$

linear polarization

$$\boldsymbol{\epsilon}^\pm_z = \mp\frac{1}{\sqrt{2}}(\boldsymbol{\epsilon}_x \pm \mathrm{i}\,\boldsymbol{\epsilon}_y)$$

circular polarization with **k** // z

dipole operator in terms of spherical harmonics

$$P^\pm_z = \boldsymbol{\epsilon}^\pm_z\cdot\mathbf{r} = \mp\frac{1}{\sqrt{2}}(x \pm \mathrm{i}y) = r\sqrt{\frac{4\pi}{3}}Y_{1,\pm1}$$

$$P^0_z = \boldsymbol{\epsilon}_z\cdot\mathbf{r} = z = r\sqrt{\frac{4\pi}{3}}Y_{1,0}.$$

The atomic transition matrix element

$$I_{\rm res} = \mathcal{A}\, |\langle b|\, P^q_\alpha |a\rangle|^2$$ dipole transition matrix element

$$|a\rangle = |R_{n,c}(r); c, m_c, s, m_s\rangle$$ initial state: core electron wavefunction

$$|b\rangle = |R_{n',l}(r); l, m_l, s, m'_s\rangle$$ final state: valence electron wavefunctions

$$R_{n,l}(r)\, Y_{l,m_l}\, \chi_{s,m_s} = |R_{n,l}(r); l, m_l, s, m_s\rangle$$ simplest wavefunctions: atomic spin orbitals of the central field form

We need to calculate the following transition matrix element:

$$\langle b|\, P^q_\alpha\, |a\rangle = \langle R_{n',l}(r); l, m_l, s, m'_s|\, P^q_\alpha\, |R_{n,c}(r); c, m_c, s, m_s\rangle$$

$$\langle b|\, P^q_\alpha\, |a\rangle = \underbrace{\delta(m'_s, m_s)}_{\text{spin}}\ \underbrace{\langle R_{n',l}(r)|r|R_{n,c}(r)\rangle}_{\text{radial}}\ \underbrace{\sum_{m_c, m_l, p} e^q_{\alpha,p}\, \langle l, m_l|\, C^{(1)}_p\, |c, m_c\rangle,}_{\text{angular}}$$

matrix elements factor into spin, radial and angular parts

$$C^{(l)}_m = \sqrt{\frac{4\pi}{2l+1}}\, Y_{l,m}(\theta,\phi)\ , \qquad \left(C^{(l)}_m\right)^* = (-1)^m C^{(l)}_{-m}\ .$$

$C_p^{(1)}$ are Racah's spherical tensor operators

Angular part of the transition matrix element

$$\underbrace{\sum_{m_c, m_l, p} e^q_{\alpha,p} \langle l, m_l | C_p^{(1)} | c, m_c \rangle,}_{\text{angular}}$$

By looking at the non-zero matrix elements we get the dipole selection rules

$$\boxed{\begin{aligned} &\Delta l = l' - l = \pm 1, \\ &\Delta m_l = m_l' - m_l = q = 0, \pm 1, \\ &\Delta s = s' - s = 0, \\ &\Delta m_s = m_s' - m_s = 0. \end{aligned}}$$

where $q\hbar$ is the X-ray angular momentum

Schematic of dipole transitions between electronic core and valence states, in the one-electron model

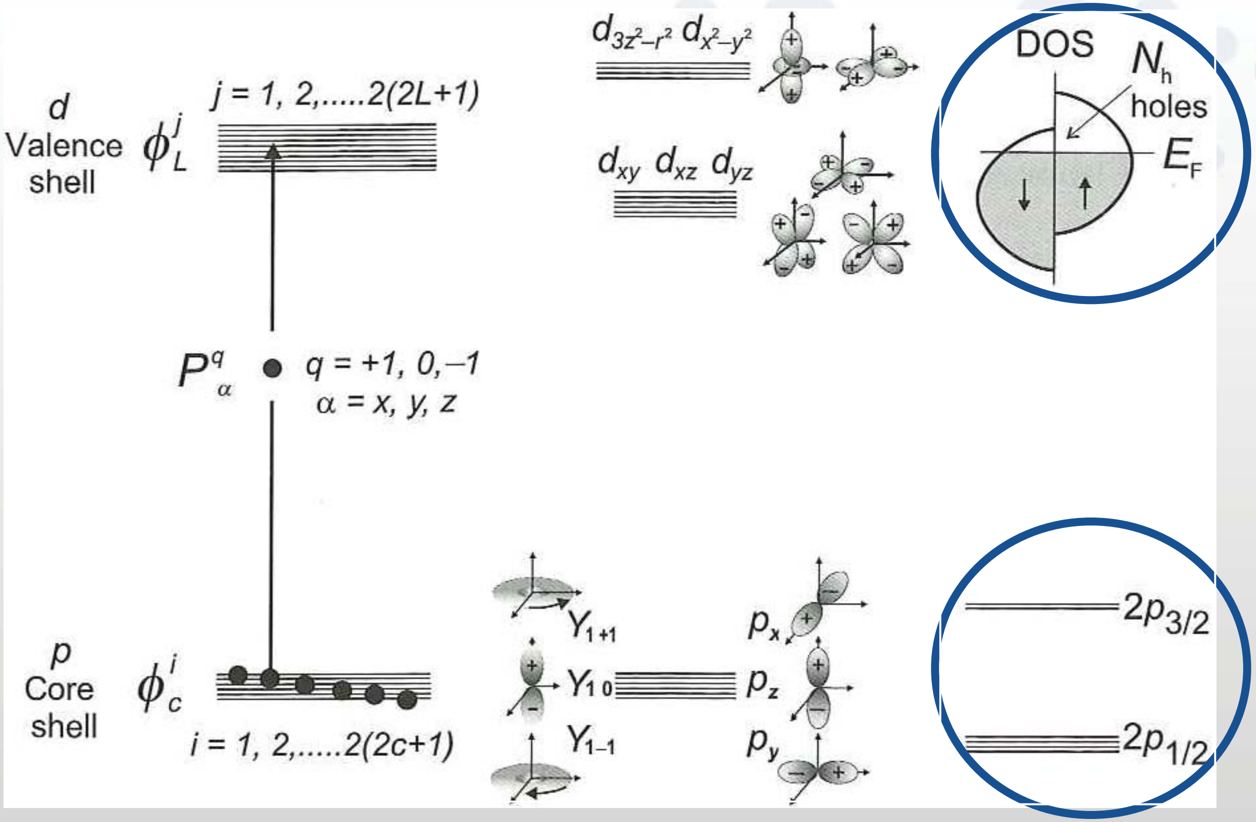

Atomic model | Ligand field model | Band model

Valence shell
spin-up / spin-down *d* states
with N_h = total number of
empty *d* states above E_F
(no. of valence holes)

Core state
spin-orbit split into $2p_{3/2}$ and
$2p_{1/2}$ states, giving rise to L_3
and L_2 edges

IMPORTANT: The sum over all basis states of a shell with angular momentum ℓ is spherically symmetric.

The sum rules

Atomic quantities such as :

1. No. of empty states or "holes" N_h per atom
2. Spin magnetic moment m_s per atom
3. Orbital magnetic moment m_o per atom

are defined by integration over the atomic volume, and are therefore isotropic quantities

Sum rules link measured intensities with valence band properties

→ Need to be sure that the measurement is angular averaged

The sum rules

- If we can measure a true "angular averaged" intensity
  - non-magnetic polycrystalline sample – any polarization
  - non-magnetic single crystals – properly averaged over all sample orientations
  - magnetic polycrystalline or single crystals: as above, but eliminating magnetic effects by saturating the sample with field parallel and antiparallel to k and summing over the two intensities
- Then we can take advantage of sum rules

Example: hole sum rule for L_2 and L_3 edges of transition metals

The intensity of the combined L_2 and L_3 resonances is directly proportional to the total number of d states above the Fermi level, i.e. the number of holes N_h in the d band.

$$\langle I_{\mathrm{L}_3} + I_{\mathrm{L}_2} \rangle = C N_{\mathrm{h}}$$

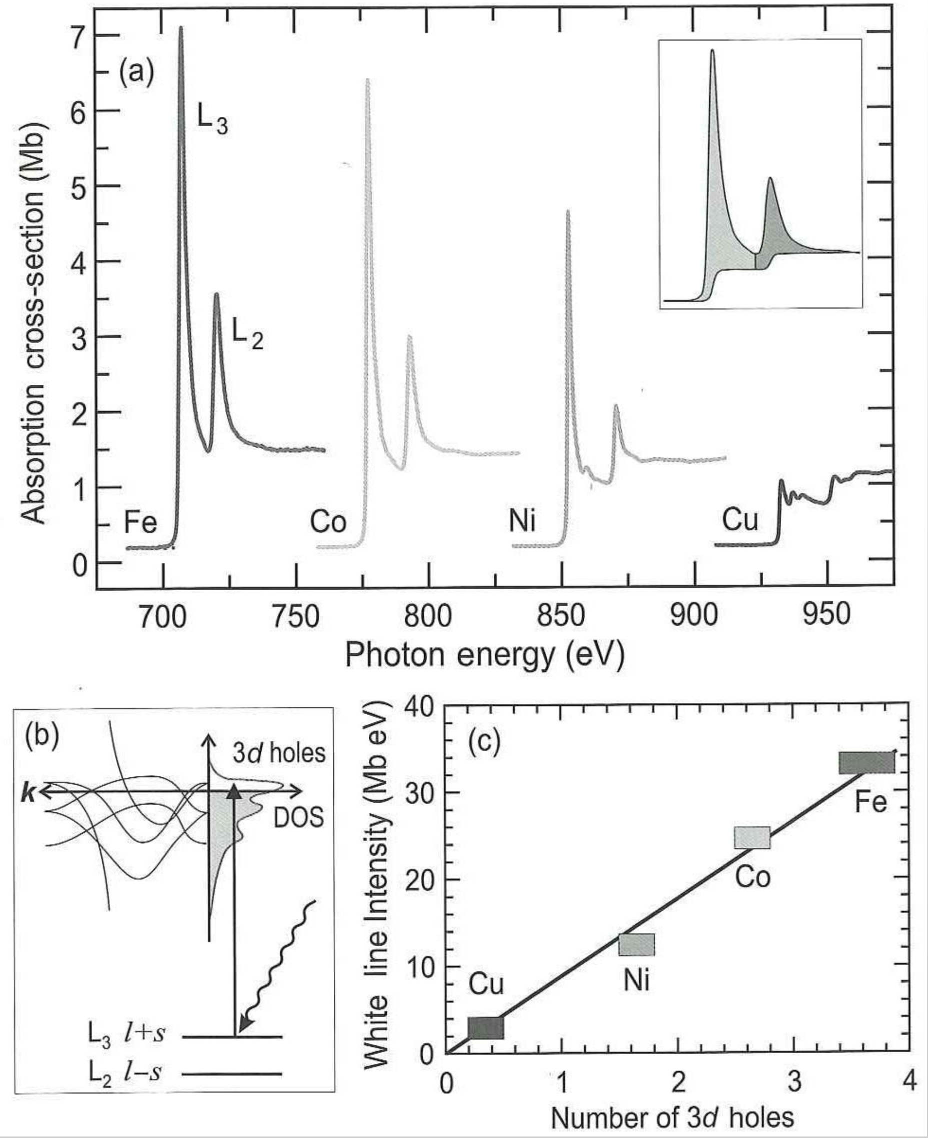

Origin of the XMCD effect

- The important intensity sum rule for the number of holes suggests that if we could make the absorption process spin-dependent, then we could measure an intensity difference that corresponds to the difference between the number of spin-up and spin-down holes, i.e. the magnetic moment.

- This can be done using circularly polarized photons and is the origin of the XMCD effect.

$$\Delta I = I^{\uparrow\downarrow} - I^{\uparrow\uparrow}$$

The XMCD intensity difference is directly proportional to the atomic magnetic moment

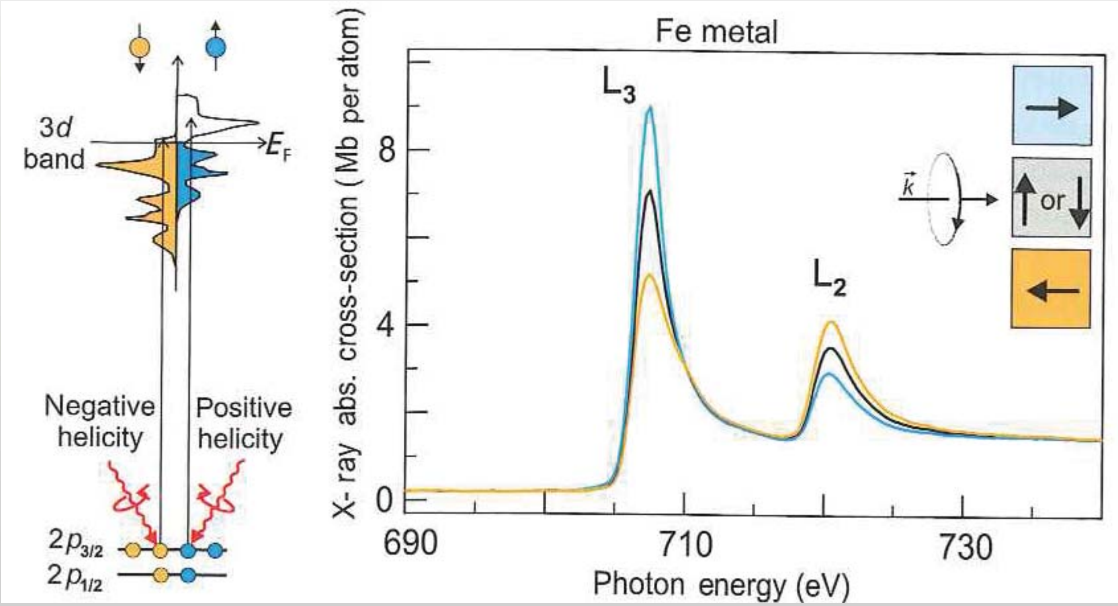

Calculation of XMCD in 3d metals: simple case filled spin-down band

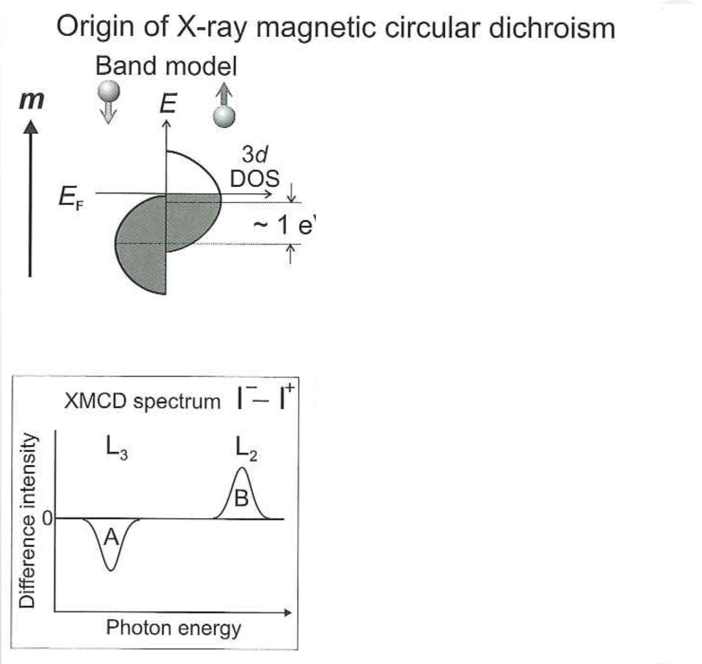

Individual squared transition matrix elements

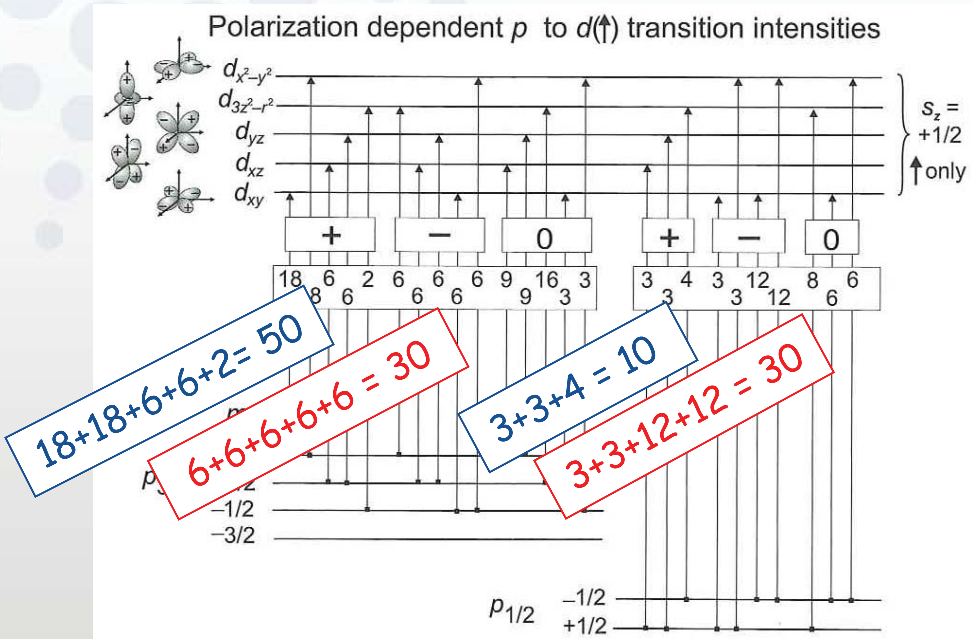

To calculate the dichroism we need to consider the angular part of the squared transition matrix element from the $p_{3/2}$ and $p_{1/2}$ states to the empty spin-up states of the d band

$$|\langle d_n, \chi^+ | \frac{P_z^q}{r} | p_j, m_j \rangle|^2$$ with index values $n = 1, \ldots, 5$, $j = 3/2, 1/2$, $m_j = \pm 3/2, \pm 1/2$ and $q = 0, \pm 1$

$$\Delta I = I^{\uparrow\downarrow} - I^{\uparrow\uparrow} = I^- - I^+$$

$$\Delta I_{L3} \sim \sum_{n,m_j} |\langle d_n, \chi^+ | C_{-1}^{(1)} | p_{3/2}, m_j \rangle|^2 - |\langle d_n, \chi^+ | C_{+1}^{(1)} | p_{3/2}, m_j \rangle|^2 \sim -20$$

$$\Delta I_{L2} \sim \sum_{n,m_j} |\langle d_n, \chi^+ | C_{-1}^{(1)} | p_{1/2}, m_j \rangle|^2 - |\langle d_n, \chi^+ | C_{+1}^{(1)} | p_{1/2}, m_j \rangle|^2 \sim +20$$

Two-step model for the XMCD intensity

Step 1

the initial state (spin-orbit split 2p band) emits spin polarized electrons (no ↑ ≠ no ↓)
→ from conservation of angular momentum

1. Spin pol opposite for X-rays with q= +1, -1
2. Spin pol opposite at L_2 and L_3 edges (opposite spin orbit coupling l+s, l-s)

Step 2

the exchange split valence shell with unequal spin up and spin down populations acts as a spin detector

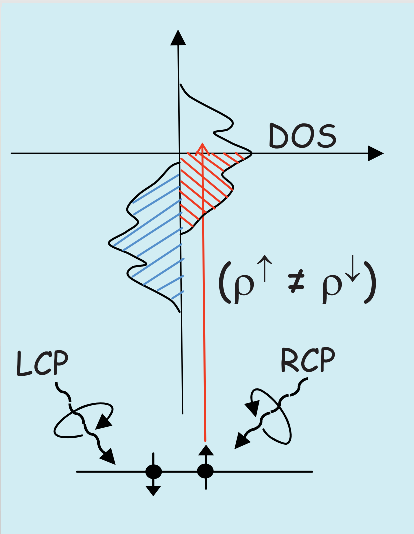

Example: L_2 edge ($2p_{1/2} \rightarrow 3d$)

q=+1: 25 % spin up, ~~75 % spin down~~

q=-1: 75 % spin up, ~~25 % spin down~~

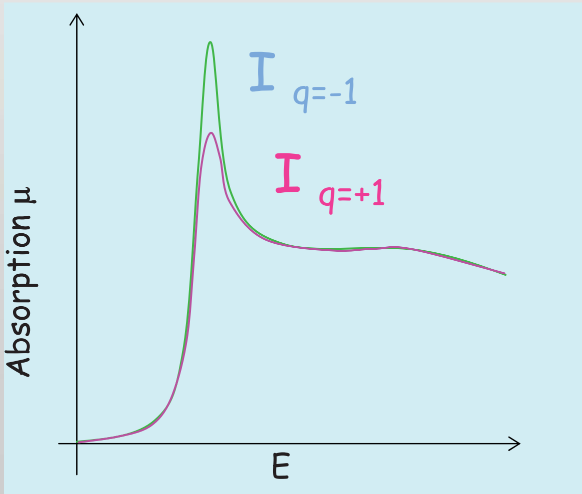

K shell dichroism

- 1s core shell has zero angular momentum → no s-o coupling → photon cannot transfer its angular momentum to the photoelectron spin (no spin polarized photoelectron) → all info goes to the photoelectron angular momentum

- 1s core shell may exhibit small splitting (exch. field or ext magn. field) $m_s = \pm \frac{1}{2}$

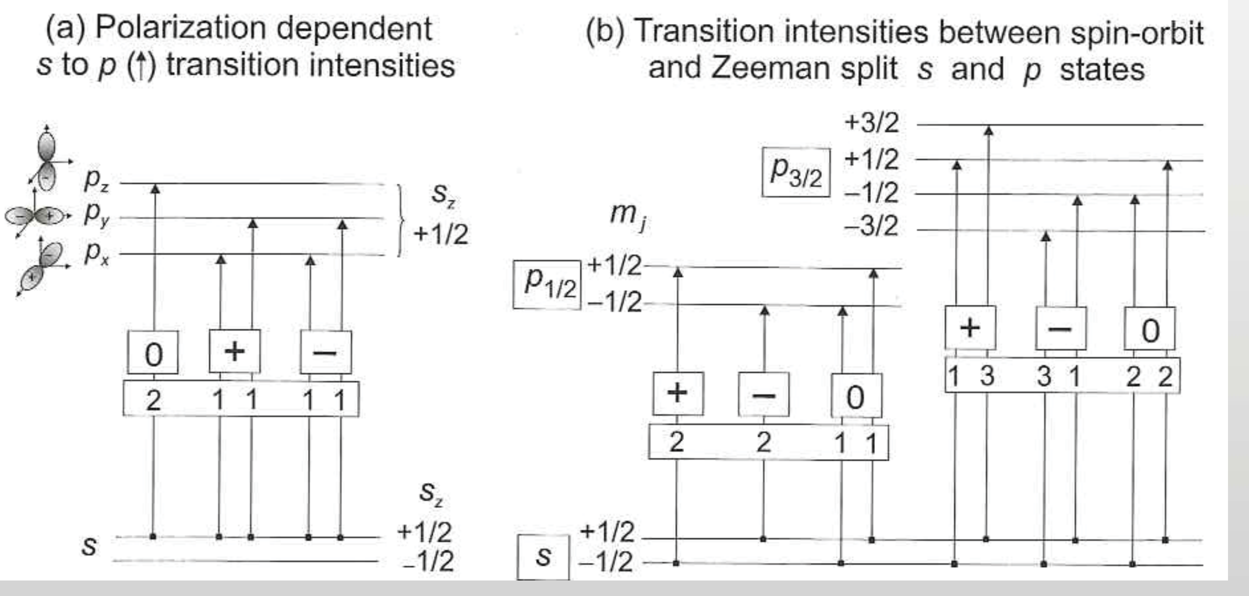

- Dichroism observed only if valence shell possess an orbital magnetic moment → valence band empty density of states must have an imbalance of states with quantum numbers $+m_l$ and $-m_l$

Quantitative determination of valence band properties

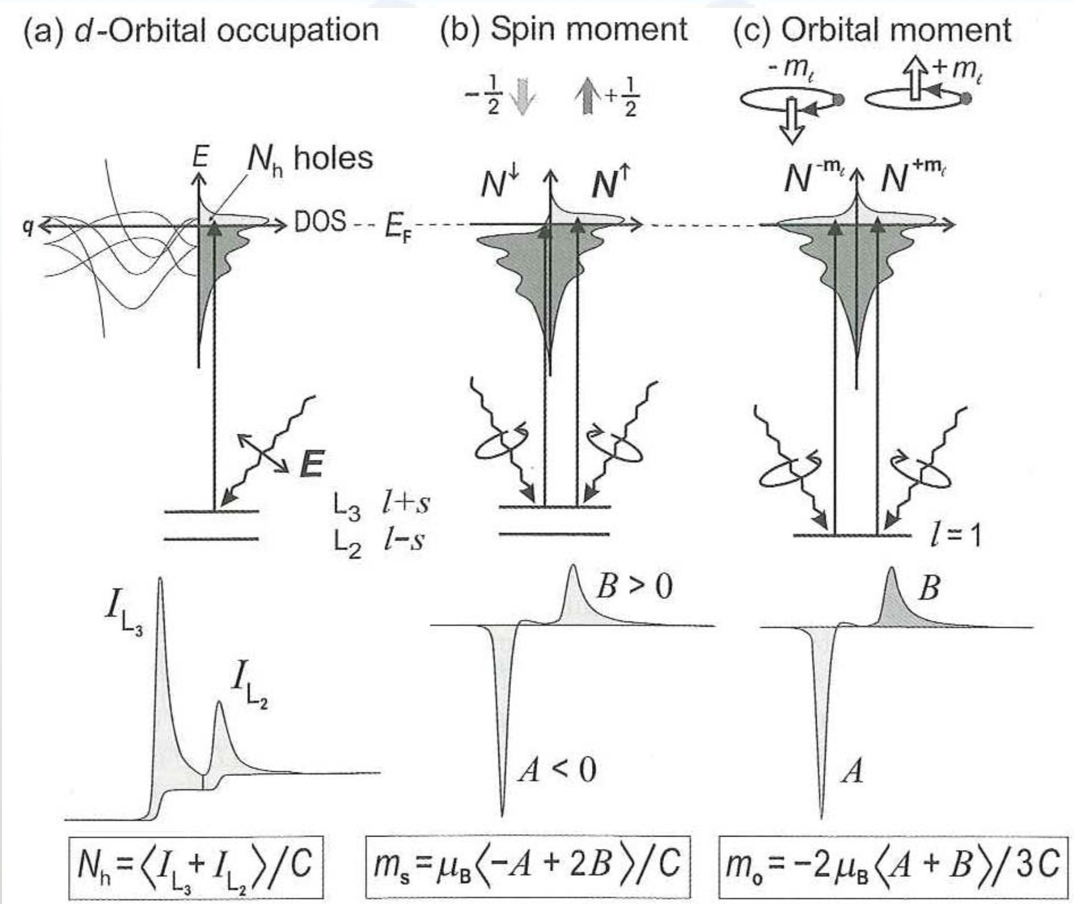

Transition intensity of core electrons into empty valence states → no. of empty valence states per atom

Dichroism intensities → size of spin moment per atom

Dichroism intensities → size of orbital moment per atom

Carra et al. PRL 70, 694 (1993)

Thole et al. PRL 68, 1943 (1992)

Anisotropy of spin moment

- We have neglected the anisotropy of the spin moment within the atom, described by the magnetic dipole operator T

$$T = \mathbf{S} - \mathbf{r}\,(\mathbf{r} \cdot \mathbf{s}) / r^2$$

- Can be induced by:
  - Anisotropic charge distribution (quadrupole moment)
    - Zero in cubic systems (isotropic charge)
    - Enhanced at surfaces and interfaces
  - Spin-orbit interaction
    - Small in 3d metals
    - Larger in 4d and 5d metals

Applications of soft XMCD:
The study of thin films magnetisation

Used properties:

1. element selectivity
2. very high sensitivity
3. sensitivity to orbital and spin magnetisation

Examples:

- Element selective hysteresis loops
- Enhanced Co orbital moments in Co/Pd multilayers
- Induced magnetic polarization across magnetic interface: Pd in Pd/Fe
- Microscopic origin of perpendicular magnetic anisotropy: from thin films to single adatom

Element specific magnetic hysteresis as a means for studying heteromagnetic multilayers

C.T. Chen et al. PRB 48 642 (1993)

Magnetic hysteresis curves by conventional techniques probe overall magnetic behaviour of the sample

- Fe/Cu/Co ML evaporated on glass
- Fluorescence yield

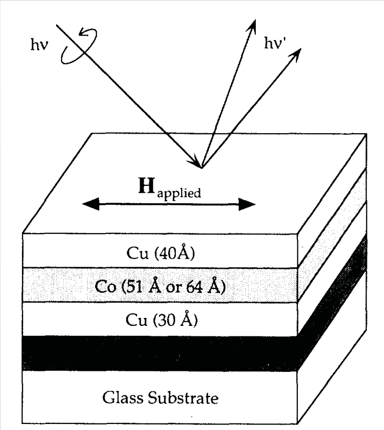

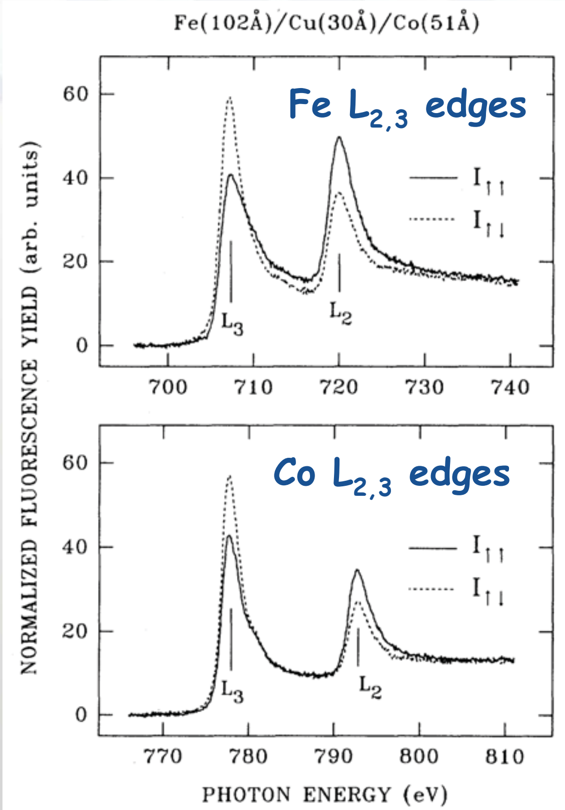

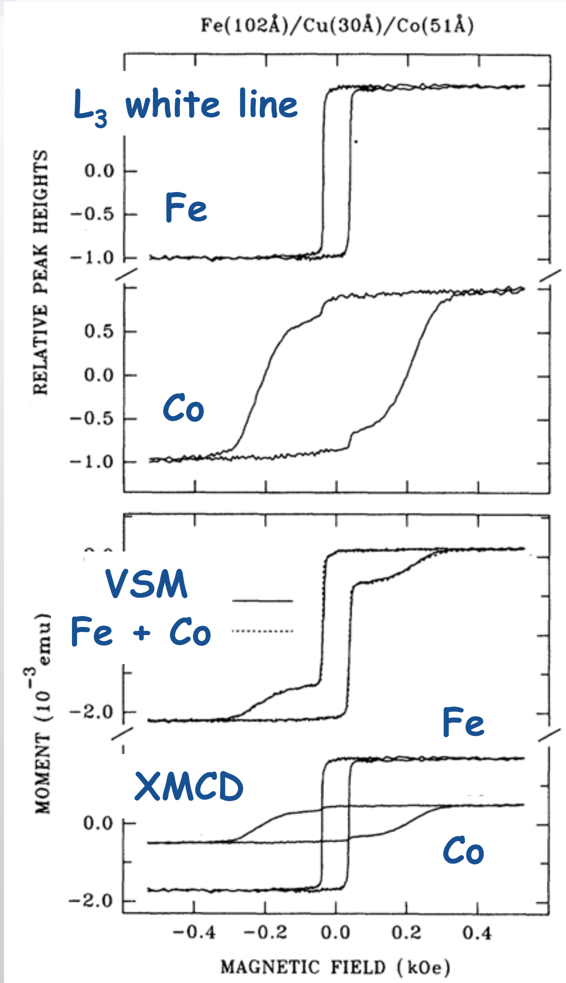

- Fe and Co curves show dramatic differences
- Fe and Co partly coupled
- VSM as linear combination of Co and Fe cycles
- Fit gives: Fe 2.1 μ_B and Co 1.2 μ_B

L_3 XMCD vs H → hysteresis loop

Giant magnetic anisotropy of single cobalt atoms and nanoparticles

Gambardella et al., Science 300, 1139 (2003)

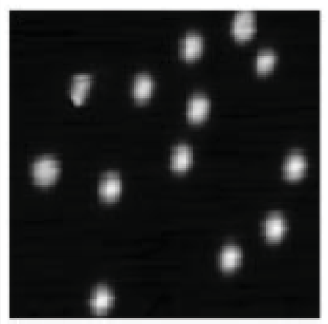

Single Co atoms on Pt(111) surface

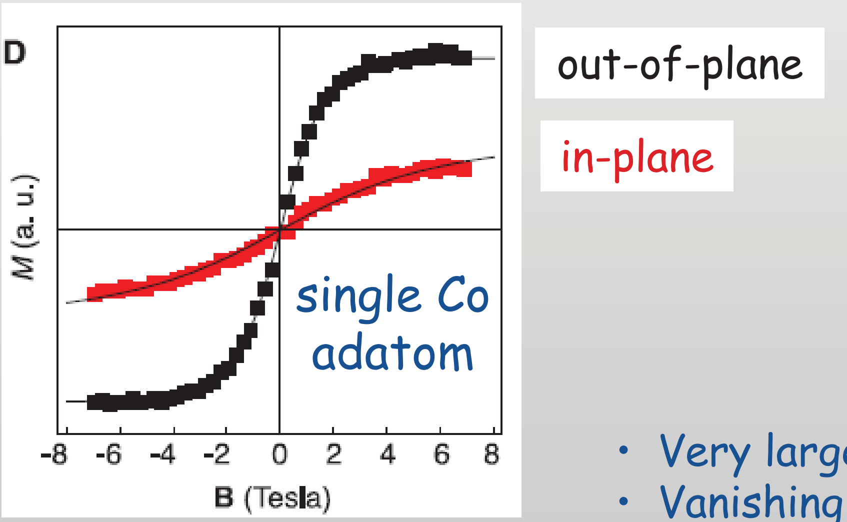

Peak of L_3 XMCD signal as f(B)

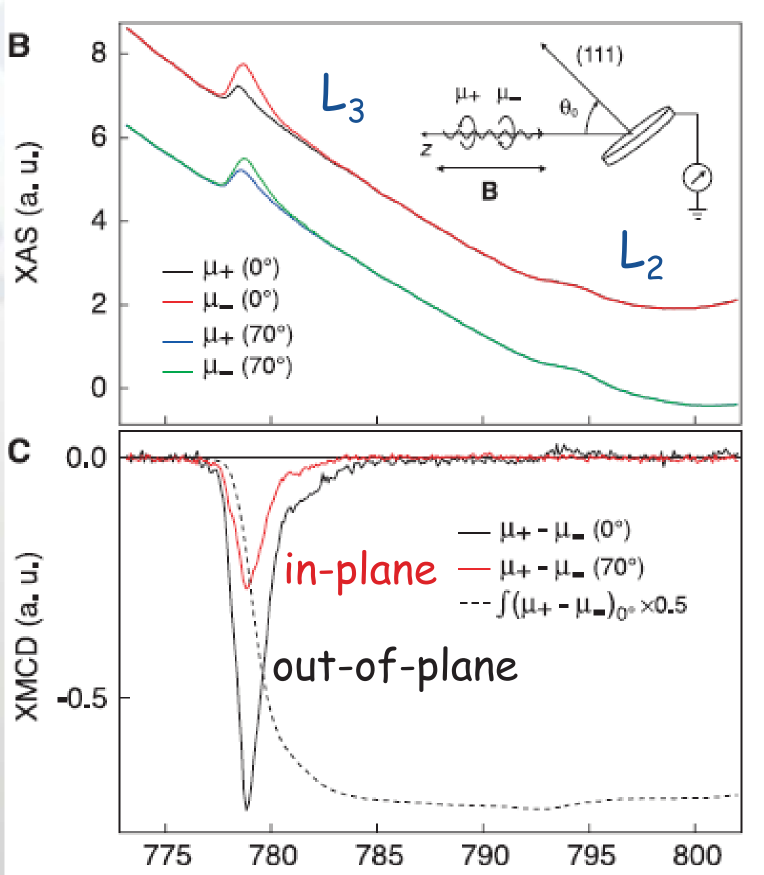

single Co adatom

- Very large L_3 XMCD → strong localized magnetic moment
- Vanishing L_2 XMCD → strong orbital magnetism
- Large in-plane and out-of-plane difference → huge MAE

Giant magnetic anisotropy of single cobalt atoms and nanoparticles

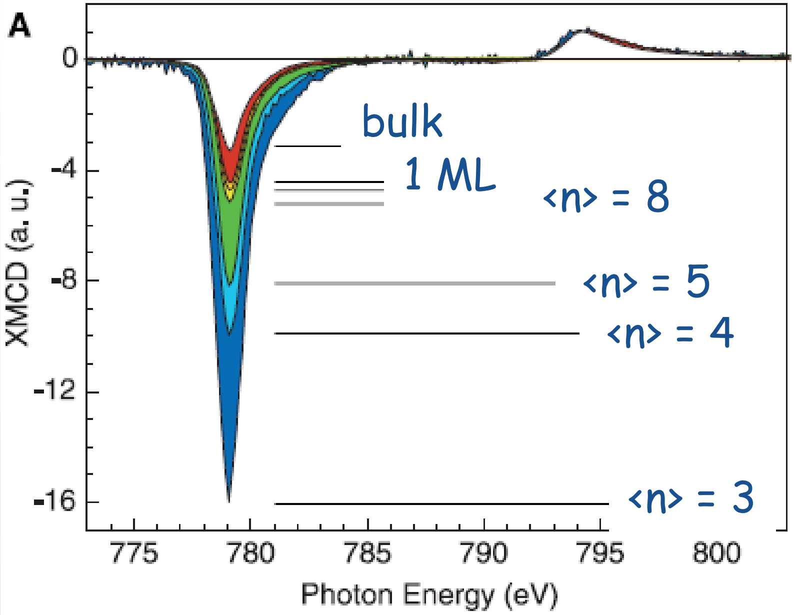

XMCD spectra as a function of average particle size <n>

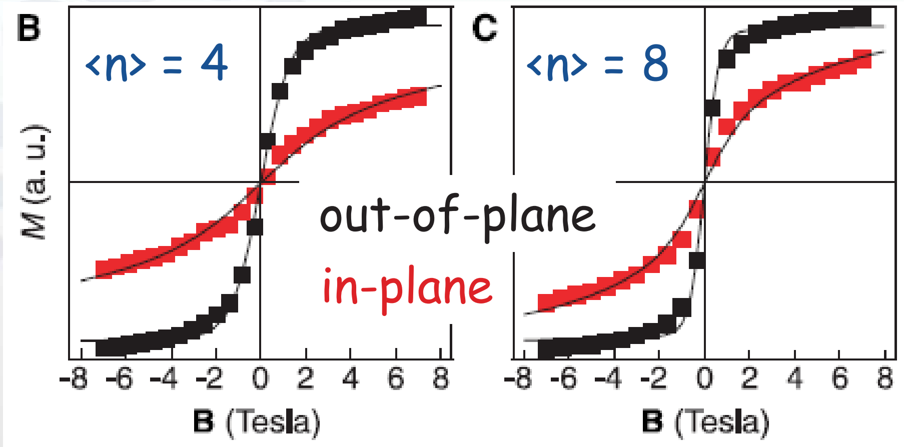

Peak of L_3 XMCD signal as f(B)

- Decrease of intensity at L_3 w/respect to L_2 with <n> → progressive quenching of orbital moment with <n>
- Decrease of MAE with <n>

Giant magnetic anisotropy of single cobalt atoms and nanoparticles

- Extremely high L :
  - reduced coordination of an isolated atom adsorbed on top of a flat surface, which favors d-electron localization and the survival of atomic-like character in the 3d orbitals
- Cannot estimate S → anisotropy of spin moment T is expected to be large and is unknown
- Exceptionally large K (MAE/atom) :
  - broken symmetry of Co adatoms as compared with the free atom
  - reduced coordination → 3d-electron localization (band narrowing) → augments s-o energy due to increase in local density of states near the Fermi level and spin magnetic moment
  - strong s-o coupling of the Pt 5d states results in additional MAE of the induced magnetization

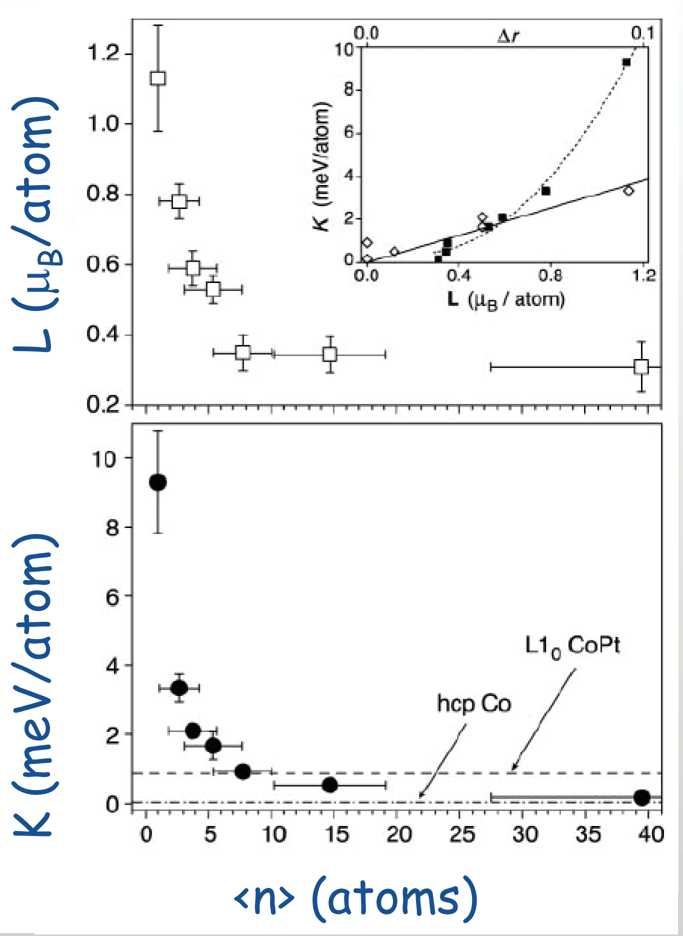

Applications of hard XMCD

Used properties:

1. element selectivity
2. high penetration depth
3. time resolution

Examples:

- Pressure induced structural and magnetic phase transitions
- Structure and magnetism at extreme magnetic fields

Pressure induced magnetic phase transitions in 3d metals and their compounds

The volume occupied by a magnetic atom drives its microscopic properties such as magnetization through its hybridization with its neighbours.

Applying pressure is the best way to modify the volume and therefore to tune hybridization. When solids are compressed, electronic bands get wider, and hybridization increases.

Reduction of distances affects band structure and can:

- modify phase stability
- induce magnetic transitions
- induce magneto-volume instabilities

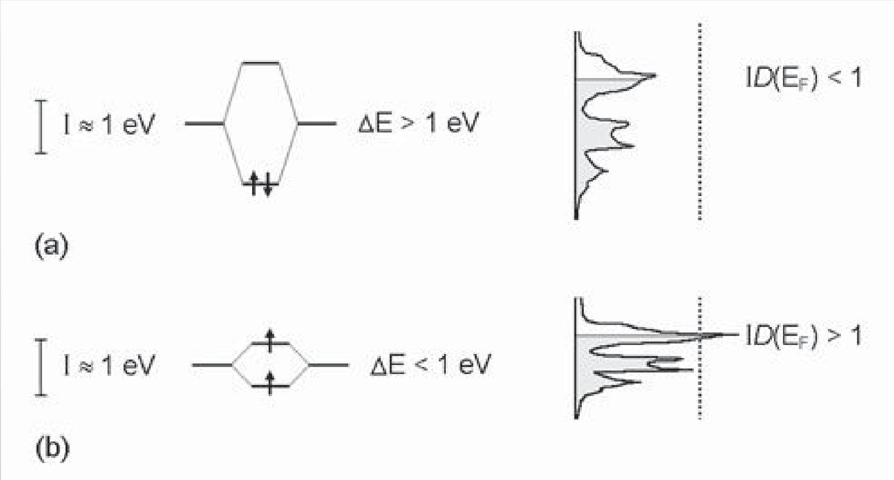

HP XMCD is an excellent tool to probe the variation of the magnetic properties with increasing hybridization between a specific atom and its neighbours.

XMCD at high pressure

- HP XMCD experiments not possible at L edges in 3d metals

  → E ~ 0.6– 1 KeV

- Become possible at K edges (E ~ 5 - 9 keV) – but difficult :

  1. K-edge XMCD is ~ 100 times smaller than at L-edge (typically ~ 10^{-3})
     - SO coupling only in final state + weak spin polarization of 4p bands
     - Indirect probe → changes of magnetic moments and ferromagnetic character as a function of external parameters (T, P, c)

  2. Comprehensive theoretical description still lacking for most systems

XMCD at high pressure

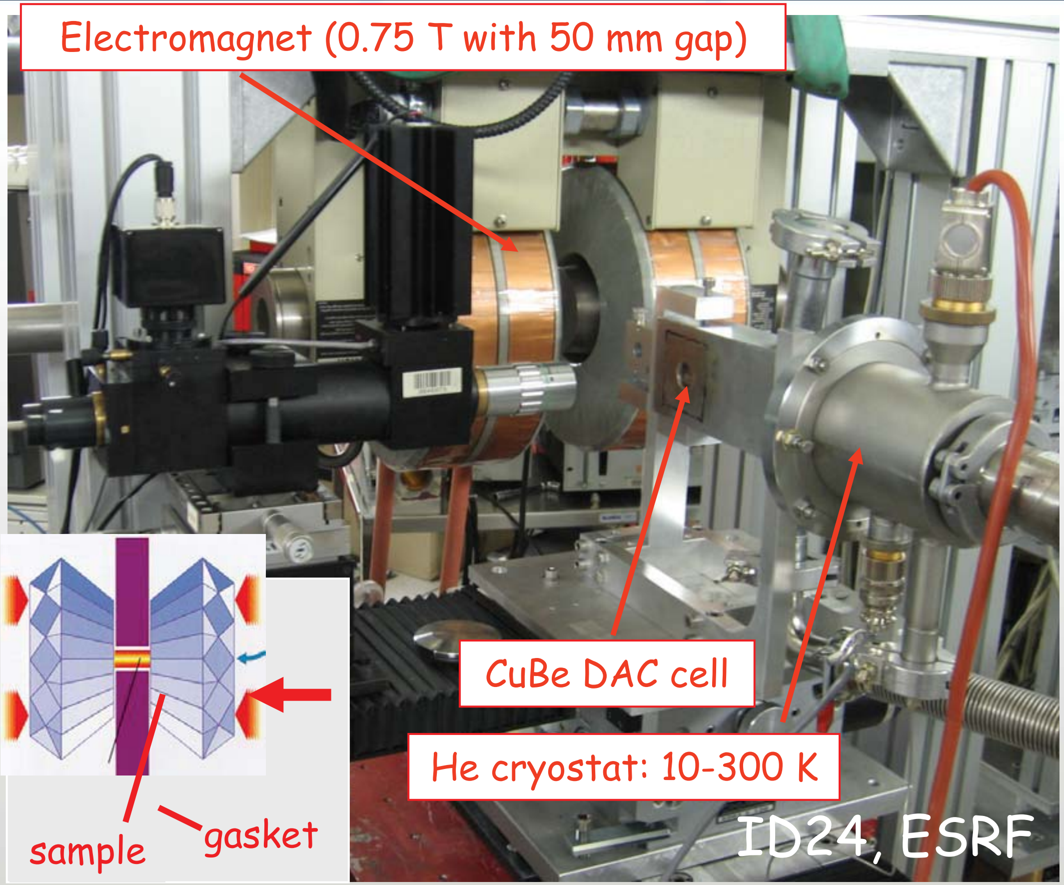

Technological challenges:

- high-flux: strong absorption from sample environment and phase plate
- spatial and spectral stability: weak signal, averaged over many acquisitions
- small focal spot: sample size < 50 μm